Journal of Alloys and Compounds, 191 (1993) 83–86
JALCOM 479

A computer assessment of the molybdenum–palladium phase diagram

R. Gürler
Institute of Metallurgy, Anadolu University, Yunusemre Kampüsü, 26470 Eskişehir (Turkey)

(Received August 6, 1992)

Abstract

The optimized phase diagram of the binary Mo–Pd system was calculated using thermodynamic coefficients derived from the assessment of available experimental phase diagram and thermodynamic data. The excess Gibbs energies of the phases are described employing the ordinary polynomial expressions in a subregular model. The temperatures of various transitions and the composition limits of the phases are reproduced satisfactorily.

1. Introduction

The assessment of the Mo–Pd system is of importance to the nuclear industry since the elements molybdenum, ruthenium, rhodium, palladium and technetium are found as single- or two-phase metallic inclusions in irradiated UO_2 and (U, Pu)O_2 nuclear fuels. Molybdenum and palladium together with ruthenium are the fission products with the major yields.

Computer assessments of several binary systems of these five elements have been made and the resulting binary Gibbs excess energy coefficients have been used successfully in multiphase diagram calculations of the elements [1–4]. In the case of the binary Mo–Pd system, there are no calculated Gibbs excess energy coefficients available and the present assessment was undertaken using experimental phase diagram and thermodynamic data to provide the best coefficients for use in higher order system constructions. The Lukas optimization program was used to obtain the best set of coefficients describing the phase diagram [5].

2. Experimental phase diagram and thermodynamic data

2.1. *Phase diagram information*

Studies of different regions of this system have been reported by various investigators. The solid state equilibria at high temperatures are generally well established as comprising a limited b.c.c. terminal solid solution of Pd in Mo, Mo(Pd) [6–8], a narrow composition range high-temperature ϵ (h.c.p.) intermediate phase [7–10] and an extensive f.c.c. solid solution of Mo in Pd, Pd(Mo) [6, 8, 9, 11]. The h.c.p. intermediate phase is formed peritectically from the Mo(Pd) solid solution at approximately 1740 °C [7, 8, 10] and decomposes eutectoidally to the b.c.c. Mo(Pd) and f.c.c. Pd(Mo) solid solutions at approximately 1400 °C [7, 8, 10]. A maximum (congruent melting point) has been reported in the liquidus of the f.c.c. Pd(Mo) solid solution [9] and this phase is most generally accepted to enter into a eutectic reaction, liquid$=\epsilon$ (h.c.p.)+f.c.c. Pd(Mo), at about 53 at.% Pd and 1775 °C [9]. A conflicting report by Savitskii *et al.* [10] indicating that the f.c.c. Pd(Mo) phase is formed peritectically from ϵ (h.c.p.) at 1710 °C has tended to be discounted in assessments of the system [12, 13], but this alternative view appears to be supported by recent studies by Kleykamp [8].

Solid state equilibria at lower temperatures (less than 1370 °C) have been reported with some uncertainty over the solubility limits of the Mo(Pd) and Pd(Mo) solid solutions and also the possible existence of intermediate phases at these lower temperatures [14–16]. However, more recent studies have shown that, at these relatively low temperatures, the system is a simple diagram with two terminal solid solutions with a mixture in between [8, 17]. The lower solid state equilibria (from 1100 to 880 °C) have been re-investigated [17] using ultra-rapidly-solidified samples and no traces of intermediate phase were found in the temperature ranges investigated. The solid solubility limit of the b.c.c. Mo(Pd) phase was found to be 2.5 at.% Pd at 1100±5 °C, 2 at.% Pd at 1050±5 °C and 0.5 at.% Pd at 900±5 °C. The f.c.c. Pd(Mo) boundary was established as 63 at.% Pd at 1100±5 °C, 65 at.% Pd at 1050±5 °C, 67.5 at.% Pd at 1000±5 °C and 72.5 at.% Pd at 900±5 °C.

0925-8388/93/$6.00

2.2. *Thermodynamic data*

Yamawaki *et al.* [18] studied the system using a calcia–zirconia solid electrolyte e.m.f. technique over the temperature range 1200–1300 K. The partial free energies, enthalpies and entropies of a solution of Mo were calculated at 1273 K. However, the uncertainties are very large for these thermodynamic properties. The partial quantities for Pd were derived at 1273 K, so as to be consistent with the phase diagram of Shunk [19]. Recently, Kleykamp [8] has re-investigated the system using a calcia–zirconia solid electrolyte e.m.f. technique over the temperature range 800–1200 K. His results are in agreement with the findings reported by Yamawaki *et al.* [18].

Kaufman and Bernstein [20] made the first attempt to calculate the diagram using the estimated Gibbs excess energy coefficients. A set of estimated equations was obtained by Brewer and Lamoreaux [12] to describe the partial thermodynamic quantities for the phases of the system. Since experimental data are available, these estimated values were not used in the assessment. Rand and Potter [2] have also tried to calculate the diagram.

3. Thermodynamic modelling

In the Lukas program the lattice stabilities of the pure elements are described by the equation

$$^{\circ}G=A-BT+CT(1-\ln T)-\tfrac{1}{2}DT^2-\tfrac{1}{2}ET^{-1}-\tfrac{1}{6}FT^3 \qquad (1)$$

In the present calculation the equations limited the first two terms and the coefficients are given in Table 1. The lattice stability values of Rand and Potter [2] were used for Pd and the lattice stability values of Andersson *et al.* [21] were used for Mo, except for the Mo(liquid) lattice stability value. It caused a problem because it was not in the correct format to employ in the Lukas optimization program and therefore a best-fit linear equation was achieved using values obtained from the original equation of the type 41 616.767 − 14.6985 + 4.035 826 × 10^{-22} T^7 [21].

TABLE 1. Gibbs energies of transformation of elements (in joules per mole). Reference states are pure solid Mo (b.c.c.) and Pd (f.c.c.)

Mo	Temperature dependence		Pd	Temperature dependence	
	1	−T		1	−T
$G^{liq}-G^{bcc}$	41402.91	14.2966	$G^{liq}-G^{fcc}$	16480	9.02
$G^{bcc}-G^{bcc}$	0	0	$G^{bcc}-G^{fcc}$	4180	−3.35
$G^{fcc}-G^{bcc}$	15200	−0.63	$G^{fcc}-G^{fcc}$	0	0
$G^{hcp}-G^{bcc}$	11550	0	$G^{hcp}-G^{fcc}$	4180	−5.86

All of the phases concerned were described using the subregular model. The ordinary polynomial expression was employed for the composition dependence of the phases and their Gibbs energies are given by the following expression

$$G_m=(1-x)_{Mo}{}^{\circ}G_{Mo}+x_{Pd}{}^{\circ}G_{Pd} +RT[(1-x)_{Mo}\ln(1-x)_{Mo}+x_{Pd}\ln x_{Pd}]+E_{G_m} \qquad (2)$$

where the excess free energy is described (for the liquid phase) as

$$E_{G_m}=(1-x)_{Mo}x_{Pd}[(366\,904.56-T193.12 -478\,773x_{Pd}+T216.85x_{Pd})] \qquad (3)$$

$(1-x)$ and x are the mole fractions of the individual components, $^{\circ}G_i$ are the lattice stability values of the pure elements and A_i are the binary polynomial coefficients which may be temperature dependent.

4. Optimization

The phase diagram data above 1373 K, from the assessed diagram [12, 13], were adopted as the main source of phase diagram data. The results of the constitutional investigation [17] were also input. The phase diagram information reported by Kleykamp [8] was only used for the b.c.c. + f.c.c. phase field because above this phase field the results contradict the assessed diagrams [12, 13]. Since, in the Lukas program, the use of contradictory data causes unreasonable results, his findings must be used separately.

The partial free energies of the elements at 1273 K, reported by Yamawaki *et al.* [18], were used. Since the exact structural states of the samples were not clearly specified an assumption was made, in the light of the present investigation, that the alloy composition at 45 at.% Pd refers to the b.c.c. + f.c.c. phase field and at 67, 78 and 87 at.% Pd refers to the f.c.c. phase field. The partial free energies of Mo measured by Kleykamp [8] at 1200 K were also used.

Initially, Rand and Potter's [2] lattice stabilities for the elements, combined with the phase diagram and thermodynamic data, were input into the Lukas program and various descriptions including regular, subregular and composition-dependent terms were tried in an effort to obtain the best coefficients producing a realistic phase diagram. All of these attempts were unsatisfactory since the f.c.c. phase reappeared in the Mo-rich part of the diagram above 1300 K, as in the binary Mo–Rh phase diagram assessment [4]. It was found that the f.c.c. phase was stable relative to the b.c.c. and h.c.p.

TABLE 2. The assessed excess Gibbs energy coefficients of the phases in the binary Mo–Pd phase diagram

Phase	Temperature dependence		Composition dependence
	1	−T	
Liquid	366904.56	193.12	1
	−478773.00	−216.85	(x_{Pd})
B.c.c.	40328.63	73.49	1
	1220269.00	159.92	(x_{Pd})
F.c.c.	71076.50	50.59	1
	−100416.81	−27.84	(x_{Pd})
H.c.p.	11387.07	16.81	1
	656.46	53.33	(x_{Pd})

phases above 1300 K. When the f.c.c. phase was removed from the calculation, the b.c.c. liquid and h.c.p. equilibria were well reproduced, thus suggesting that the Mo f.c.c. phase stability term was causing the problem. The Mo lattice stabilities from Andersson *et al.* [21] were therefore tried after the modification of the format of the Mo(liquid) phase stability equation. These stabilities proved to be satisfactory and after some attempts the coefficients best describing the phase diagram were obtained. These coefficients are shown in Table 2. The temperature dependence of the Gibbs excess energy of the phases is given in Table 2 together with the composition dependence. An example of this is provided in eqn. (3).

5. Results and discussion

The diagram above 1000 K, plotted using the assessed coefficients, is compared with the experimental diagram in Fig. 1. As can be seen, agreement with the experimental diagram is generally very satisfactory. The intricate details around 2000 K are also reproduced very satisfactorily in accordance with the experimental diagram and are illustrated in Fig. 2. The calculated diagram comprises three reactions (eutectic, peritectic, eutectoid) and a congruent melting point and their temperatures are reproduced near or within the experimental error limits reported. The temperature dependence of the b.c.c. and f.c.c. phase limits are calculated quite well. The equilibria involving the liquid phase are also produced satisfactorily, although no thermodynamic data were available. The similarity of the temperature transitions and composition limits of the phases around the complicated region shows that the subregular model can be applied successfully to reproduce a complex area without any need for additional terms.

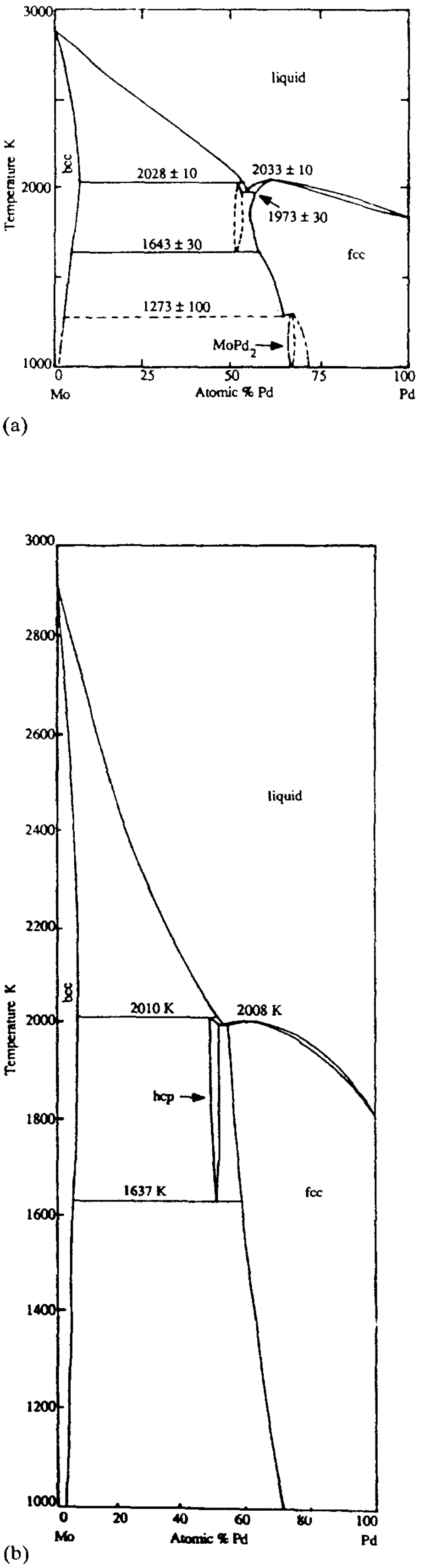

(a)

(b)

Fig. 1. Phase diagrams: (a) plotted using experimental data and (b) plotted using assessed coefficients.

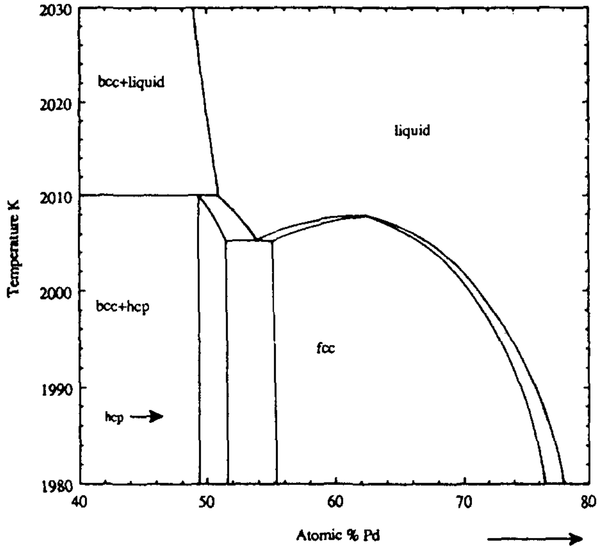

Fig. 2. Peritectic and eutectic region of the phase diagram displayed in more detail.

TABLE 3. Comparison of the present assessed integral molar free energies with those reported by Kleykamp [8] at 1200 K and Yamawaki *et al.* [18] at 1273 K

x_{Pd}	ΔG, 1200 K (J mol^{-1})		x_{Pd}	ΔG, 1273 K (J mol^{-1})	
	Current calc.	Kleykamp		Current calc.	Yamawaki
0.975	−2107	−3000	0.870	−7648	−7531
0.950	−3714	−5000	0.785	−9551	−9623
0.925	−5042	−6300	0.670	−9581	−7950
0.900	−6142	−7200			
0.850	−7764	−8800			
0.800	−8719	−9800			
0.750	−9100	−10400			
0.700	−8981	−10600			

The partial Gibbs energies of Mo derived at 1200 K from the present calculated coefficients are shown in Fig. 3 with the experimental values reported by Yamawaki *et al.* [18] and Kleykamp [8]. The integral Gibbs energies are compared in Table 3. As can be seen the agreement with the experimental values is very satisfactory.

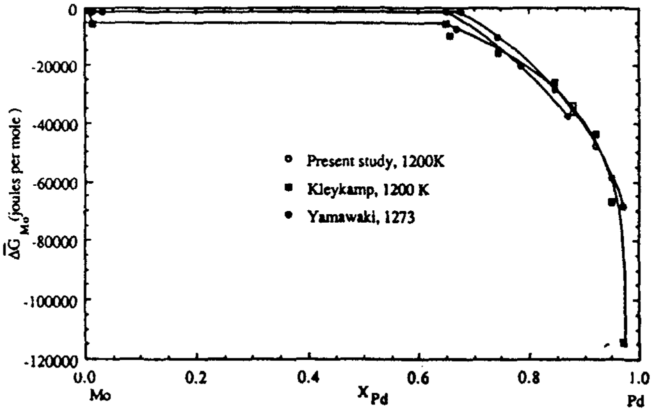

Fig. 3. Comparison of the calculated partial free energies of Mo with the experimental values at 1200 and 1273 K.

References

1 H. R. Haines, P. E. Potter and M. H. Rand, in *Proc. IAEA Symp. on Thermodynamics of Nuclear Materials, July, 1979,* Vol. 1, IAEA, Vienna, Austria, 1980, p. 471.
2 M. H. Rand and P. E. Potter, *Phys. Rev. B., 103* (1981) 21.
3 R. Gürler, *PhD Thesis,* University of Birmingham, 1990.
4 R. Gürler and J. N. Pratt, *J. Alloys Comp. 189,* (1992) 97.
5 Lukas, E. Th. Henig and B. Zimmerman, *Calphad, 1* (1977) 225.
6 E. Raub, *Z. Metallkd., 45* (1954) 23.
7 C. W. Haworth and W. Hume-Rothery, J. Inst. Met., 87 (1958–1959) 265.
8 H. Kleykamp, *J. Nucl. Mater., 167* (1989) 49.
9 E. Anderson, *J. Less-Common Met., 6* (1964) 81.
10 E. M. Savitskii, M. A. Tylkina and O. Kh. Khamidor, *Russ. J. Inorg. Chem., 9* (1964) 1745.
11 W. Zaiss, S. Steeb and T. Krabichler, *Z. Metallkd., 63* (1972) 180.
12 L. Brewer and R. H. Lamoreaux, *Atomic Energy Review Special Issue No. 7,* IAEA, Vienna, 1980.
13 T. B. Massalski, *Binary Alloy Phase Diagrams,* American Society for Metals, Metals Park, OH, 1986.
14 L. A. Cornish, *PhD Thesis,* Birmingham University, 1985.
15 P. Greenfield and P. A. Beck, *Trans. AIME, 206* (1959) 265.
16 A. Maldonado and K. Schubert, *Z. Metallkd., 55* (1964) 619.
17 R. Gürler and J. N. Pratt, *J. Less-Common Met., 175* (1991) 71.
18 M. Yamawaki, Y. Nagai, T. Kogai and M. Kanno, in *Proc. IAEA Symp. on Thermodynamics of Nuclear Materials, July, 1979,* Vol. 1, IAEA, Vienna, Austria, 1980, p. 249.
19 F. A. Shunk, *Constitution of Binary Alloys,* Second Supplement, McGraw-Hill, 1969.
20 L. Kaufman and H. Bernstein, *Computer Calculation of Phase Diagrams,* Academic Press, New York, 1970.
21 J. O. Andersson, A. Fernandez Guillermet and P. Gustafson, *TRITA-MAC-0319* (Oct. 1986), Royal Institute of Technology, Stockholm.